Peer-reviewed version available at Earth and Planetary Science Letters 2018, 485, 9-18; doi:10.1016/j.epsl.2017.12.025

Subterranean Karst Environments as a Global Sink for Atmospheric Methane

Kevin D. Webster[1,2], Agnieszka Drobniak[3], Giuseppe Etiope[4,5], Maria Mastalerz[3], Peter E. Sauer[6] and Arndt Schimmelmann[6]

[1]School of Natural Resources and the Environment, University of Arizona, 1064 E Lowell St, Tucson, Arizona 85721, USA

[2]Department of Ecology and Evolutionary Biology, University of Arizona, 1041 E Lowell St, Tucson, Arizona 85721, USA.

[3]Indiana Geological Survey, Indiana University, 611 North Walnut Grove Ave., Bloomington, Indiana 47405, USA.

[4] Istituto Nazionale di Geofisica e Vulcanologia, Sezione Roma 2, Italy.

[5] Faculty of Environmental Science and Engineering, Babes-Bolyai University, Cluj-Napoca, Romania.

[6] Department of Earth and Atmospheric Sciences, Indiana University, 1001 E 10th St. Bloomington, IN 47405, USA.

* corresponding author: kevdwebs@email.arizona.edu; telephone: 520-621-2539.

Keywords: cave; greenhouse gas; karst; methane; methanogenesis; methanotrophy

Peer-reviewed version available at Earth and Planetary Science Letters 2018, 485, 9-18; doi:10.1016/j.epsl.2017.12.025

Abstract

The air in subterranean karst cavities is often depleted in methane (CH_4) relative to the atmosphere. Karst is considered a potential sink for the atmospheric greenhouse gas CH_4 because its subsurface drainage networks and solution-enlarged fractures facilitate atmospheric exchange. Karst landscapes cover about 14% of earth's continental surface, but observations of CH_4 concentrations in cave air are limited to localized studies in Gibraltar, Spain, Indiana (USA), Vietnam, Australia, and by incomplete isotopic data. To test if karst is acting as a global CH_4 sink, we measured the CH_4 concentrations, $\delta^{13}C_{CH_4}$, and $\delta^{2}H_{CH_4}$ values of cave air from 33 caves in the USA and three caves in New Zealand. We also measured CO_2 concentrations, $\delta^{13}C_{CO_2}$, and radon (Rn) concentrations to support CH_4 data interpretation by assessing cave air residence times and mixing processes. Among these caves, 35 exhibited subatmospheric CH_4 concentrations in at least one location compared to their local atmospheric backgrounds. CH_4 concentrations, $\delta^{13}C_{CH_4}$, and $\delta^{2}H_{CH_4}$ values suggest that microbial methanotrophy within caves is the primary CH_4 consumption mechanism. Only 5 locations from 3 caves showed elevated CH_4 concentrations compared to the atmospheric background and could be ascribed to local CH_4 sources from sewage and outgassing swamp water. Several associated $\delta^{13}C_{CH_4}$ and $\delta^{2}H_{CH_4}$ values point to carbonate reduction and acetate fermentation as biochemical pathways of limited methanogenesis in karst environments and suggest that these pathways occur in the environment over large spatial scales. Our data show that karst environments function as a global CH_4 sink.

Peer-reviewed version available at Earth and Planetary Science Letters 2018, 485, 9-18; doi:10.1016/j.epsl.2017.12.025

1. Introduction

Atmospheric methane (CH_4) is a greenhouse gas and its concentration is increasing in the atmosphere (Dlugokencky et al., 2011; Sussmann et al., 2012; Ciais et al., 2013). The present globally averaged CH_4 concentration is 1.87 ppmv which is 2.5 times higher than preindustrial levels (Nisbet et al., 2016). The increase in atmospheric CH_4 is due to an imbalance between CH_4 sources and sinks. Anthropogenic and natural sources combine to contribute about 680 Tg a^{-1} of CH_4 to the atmosphere while reactions with hydroxyl (·OH) and chlorine radicals in the troposphere and stratosphere remove about 600 Tg a^{-1} (Kirschke et al., 2013). Methanotrophic consumption in soils, the next largest sink, removes 30 Tg a^{-1} (Kirschke et al., 2013). Despite improvements in estimating individual sources and sinks of atmospheric CH_4, the associated errors remain large (Kirschke et al., 2013). Recent studies suggest that caves may act as an additional CH_4 sink (Mattey et al., 2013; Fernandez-Cortes et al., 2015; McDonough et al., 2016; Webster et al., 2016; Lennon et al., 2017).

Caves and associated karst landscapes may be an important overlooked sink for atmospheric CH_4 because they are estimated to cover as much as 10 to 20 % of the continental surface with more precise estimates suggesting about 13.8 % (Palmer, 1991; Ford and Williams, 2007). Karst landscapes are frequently associated with the chemical dissolution of limestones, but can form in any soluble rock body. The resulting caves, solution-enlarged fractures, and internal drainage networks that function to transport mass from high elevations to low elevations also allow for subsurface-surface atmospheric exchange (Kowalczk and Froelich, 2010; Garcia-Anton et al., 2014). The total volume and surface area of karst conduits able to interact with the atmosphere is unknown, in part due to small fractures and the difficulty of imaging the subsurface with

64 geophysical methods. Karst caves, due to their accessibility, provide opportunities for non-
65 invasive, *in-situ* analyses and sampling.

66 Cave and karst landscapes form in two common ways, each of which influences karst's
67 capacity to act as a CH_4 sink. Epigenic karst forms through the interaction of limestone with
68 carbonic acid derived from the dissolution of atmospheric and soil CO_2 into surface waters. By
69 contrast, hypogenic caves form when corrosive water from deep sources migrates into and
70 dissolves limestone bedrock. Epigenic caves are more widespread, and atmospheric to
71 subatmospheric CH_4 concentrations of 1.8 ppmv to < 0.1 ppmv have been observed in these
72 settings (Mattey et al., 2013; Fernandez-Cortes et al., 2015; McDonough et al., 2016; Webster et
73 al., 2016; Lennon et al., 2017). For comparison, in some hypogenic caves elevated CH_4
74 concentrations from 2 ppmv to 1 % have been observed in association with CH_4-rich springs or
75 seeps related to fluid migration from deep hydrocarbon-bearing sedimentary rocks, i.e. seepage
76 processes that are widespread on Earth (Sarbu et al., 1996; Hutchens et al., 2004; Jones et al., 2012;
77 Webster et al., 2017). The dominance of epigenic karst suggests these regions are functioning as a
78 CH_4 sink at the global scale, but more observations are needed.

79 Different hypotheses have been put forward to explain the low CH_4 concentrations
80 observed in epigenic cave air. The combination of subatmospheric CH_4 concentrations and the
81 stable carbon isotopic ratio of CH_4 in the air of caves in Gibraltar led to the hypothesis that
82 microorganisms were responsible for the removal of CH_4 (Mattey et al., 2013). In turn, low CH_4
83 concentrations in Spanish caves, in the presumed absence of CH_4-consuming (methanotrophic)
84 bacteria, led to the hypothesis that CH_4 oxidation was induced by ions and ·OH generated by the
85 radioactive decay of radon and daughter nuclides (Fernandez-Cortes et al., 2015). Since these
86 initial observations, datasets from caves in Australia, the USA, and Vietnam have pointed towards

methanotrophic CH_4 oxidation (McDonough et al., 2016; Webster et al., 2016; Lennon et al., 2017, Waring et al., 2017).

The chemical composition of cave air results from the mixing of the atmosphere and air from the overlying soils and epikarst. These processes should also influence the CH_4 concentrations of cave air. Previous studies have shown that CH_4 concentrations have been inversely correlated with CO_2 concentrations in cave air (Mattey et al., 2013; Ferndandez-Cortes et al., 2015; McDonough et al., 2016; Webster et al., 2016). Cave air CO_2 concentrations are positively correlated with radon (Rn) concentrations and Rn is known to track cave air residence time (Cunningham and LaRock, 1991; Batiot-Guilhe et al., 2007; Kowalczk and Froelich, 2010; Mattey et al., 2010; Gregorič et al., 2011, 2014). Additionally, the stable C isotope composition of CO_2 ($\delta^{13}C_{CO_2}$), can track the sources of CO_2 in the environment. For example, $\delta^{13}C_{CO_2}$ values of −24 ‰ are associated with soil CO_2, while atmospheric CO_2 has $\delta^{13}C_{CO_2}$ values ranging from −8.5 ‰ to −10 ‰ (Amundson et al., 1998; Keeling et al., 2010; Peyraube et al., 2013). Thus CO_2, Rn, and $\delta^{13}C_{CO_2}$ in cave air can help determine the influence of cave air mixing processes on CH_4.

The stable C and H isotope compositions of CH_4 ($\delta^{13}C_{CH_4}$ and $\delta^{2}H_{CH_4}$) also provide tools for understanding the sources and sinks of CH_4 in caves because different CH_4 sources are associated with characteristic $\delta^{13}C_{CH_4}$ and $\delta^{2}H_{CH_4}$ values. For example, CH_4 produced from carbonate reduction has $\delta^{13}C_{CH_4}$ and $\delta^{2}H_{CH_4}$ values that range from −112 to −60 ‰ VPDB and from −350 to −100 ‰ VSMOW respectively (Whiticar, 1999). Atmospheric CH_4 has $\delta^{13}C_{CH_4}$ and $\delta^{2}H_{CH_4}$ values around −47.5 and −100 ‰ (Miller et al., 2002; Townsend-Small et al., 2012). The $\delta^{13}C_{CH_4}$ and $\delta^{2}H_{CH_4}$ values of CH_4 can also be altered through secondary processes such as oxidation and mixing. The oxidation pathways of CH_4 by methanotrophs or the ·OH have

fractionation factors that cause the residual CH_4 to show increases in $\delta^2H_{CH_4}$ values of 8.5 ‰ for every 1 ‰ increase in $\delta^{13}C_{CH_4}$ value and increases in $\delta^2H_{CH_4}$ values of 72 ‰ for every 1 ‰ increase in $\delta^{13}C_{CH_4}$ value, respectively (Feisthauer et al., 2011; Saueressig et al., 2001). Mixing between two different CH_4 sources creates a linear trend between the two members. Thus, measuring the $\delta^{13}C_{CH_4}$ and $\delta^2H_{CH_4}$ of cave air should allow for the determination of cave air CH_4 sources.

The objective of the present work is to extend the karst CH_4 dataset and test the hypothesis that karst systems act as a CH_4 sink on a global scale. To this aim, we studied CH_4 concentrations, $\delta^{13}C_{CH_4}$, and $\delta^2H_{CH_4}$ in cave air from 33 epigenic caves in the USA and three epigenic caves in New Zealand. CO_2, $\delta^{13}C_{CO_2}$, and Rn were also measured to support CH_4 data interpretation *via* assessing cave air residence times and mixing processes. Data analysis is focused on determining CH_4 concentrations, origin, mixing processes and isotopic fractionations.

2. Methods

2.1. Sampling and analyses

Air samples from the study caves were collected over a timespan of roughly four years (Fig. 1; Table 1). Study caves fell into three broad groups, those from the Appalachian fold and thrust belt (16); those in gently warped intracratonic basins of the USA (17); and those from the North Island of New Zealand (3). Cave air was sampled using *in-situ* and discrete methods. *In-situ* CH_4, CO_2, and Rn abundance analyses were carried out using a suite of instruments (Table 2). Discrete samples of cave air were collected in pre-evacuated 50-mL serum vials, in 1 to 3-L Tedlar® bags, or in 4-L glass bottles. CH_4 and CO_2 concentrations of discrete samples were measured *via* gas chromatography.

We assessed cave air mixing processes through a variety of techniques. A qualitative estimate on cave air residence time was obtained by comparing CH_4 to CO_2 concentrations at individual locations in each cave. Additionally, we measured the Rn concentrations of caves 32 through 36 to assess the relationship between cave air residence time, CH_4 concentrations, and CO_2 concentrations. $\delta^{13}C_{CO_2}$ data were used to assess the sources of CO_2 and thus of air entering the caves. We also assessed the distance from each sampling location to cave entrances as another tool to understand cave air mixing processes.

CH_4 and CO_2 concentrations from discrete air samples were measured at Indiana University using a Varian 450 gas chromatograph (GC) (Varian – Agilent Technologies, Palo Alto, California). The GC was fitted with a flame ionization detector (FID) for CH_4 and a thermal conductivity detector (TCD) for CO_2. Standard gas mixtures from Air Liquide America Specialty Gasses LLC (Plumsteadville, Pennsylvania) were used for 3-point calibration curves to convert signals measured on the GC to concentrations. CH_4 standards measured on the GC had errors of ± 5 to ± 14 % of the reported concentrations. CH_4 concentrations are reported with the uncertainty associated with the standard curve unless the calculated uncertainty was ≤ 0.1 ppmv. Samples with calculated uncertainties ≤ 0.1 ppmv were assigned uncertainties of 0.1 ppmv based on replicate measurements. The uncertainty associated with standard curves for CO_2 concentrations varied from < ± 1 to 5 %. CO_2 concentrations were assigned uncertainties based on their associated standard curve.

The stable carbon isotope ratios of CH_4 and CO_2 and hydrogen stable isotope ratios of CH_4 were measured on a ThermoFinnigan Delta Plus XP mass spectrometer in the Stable Isotope Research Facility at Indiana University. Carbon stable isotope ratios are expressed as conventional $\delta^{13}C_{CH_4}$ and $\delta^{13}C_{CO_2}$ values in ‰ along the scale anchored to Vienna Pee Dee Belemnite (VPDB).

Hydrogen stable isotope ratios are expressed as $\delta^2H_{CH_4}$ values in ‰ along the scale anchored to Vienna Standard Mean Ocean Water (VSMOW). CH_4 samples were measured in continuous-flow mode using CH_4 preconcentration, cryofocusing (Miller et al., 2002), and a gas chromatography-oxidation/pyrolysis-isotope ratio mass spectrometer (GC-ox/pyr-IRMS) interface. Varying sample extraction times were used to isolate roughly 0.45 and 0.90 μmol of CH_4 prior to the introduction of the sample to the GC-ox/pyr-IRMS for analysis of $\delta^{13}C_{CH_4}$ and $\delta^2H_{CH_4}$ values, respectively. In-house CH_4 standards methane #3, methane #6, and methane ALM with $\delta^{13}C_{CH_4}$ and $\delta^2H_{CH_4}$ values of [+19.86 ± 0.05; +2.2 ± 1.2] ‰, [−39.40 ± 0.02; −153 ± 2] ‰, and [−58 ± 1; −272.2 ± 3.4] ‰ were used for 2-point normalizations. Errors associated with $\delta^{13}C_{CH_4}$ and $\delta^2H_{CH_4}$ values were calculated using a standard curve that accounted for the peak size of the measurement. Analytical repeatability of internal standards ranged from 0.14 to 0.6 ‰ for $\delta^{13}C_{CH_4}$ and from to 7 to 18 ‰ for $\delta^2H_{CH_4}$.

$\delta^{13}C_{CO_2}$ values were measured in continuous-flow mode using a GasBench II inlet (Tu et al., 2001). Measured $^{13}C/^{12}C$ ratios of CO_2 from cave air were converted to the VPDB scale using a single isotopically characterized in-house standard that has a value of 12.0 ± 0.2 ‰.

2.2 Data elaboration and quality control

In-situ measurements were preferentially used when statistically analyzing gas concentration data. When *in-situ* measurements were not available, concentrations measured on the GC were used in the statistical analyses. Samples and data were screened for quality control by comparing the samples with *in-situ* measurements and visual estimation of the volume of sample bags. If a sample bag had been shown to exhibit a leak for one analyte, data from that

sample were discarded. CH_4 and CO_2 concentrations measured by both GC-FID and FTIR showed strong agreements ($GC(CO_2) = 0.92 \pm 0.04 * FTIR(CO_2) + 100 \pm 300$, $r^2 = 0.99$, $p = 5*10^{-19}$; $GC(CH_4) = 0.7 \pm 0.2 * FTIR(CH_4) + 0.2 \pm 0.2$, $r^2 = 0.62$), and the stable isotopic composition of the samples was not related to their storage time ($\delta^{13}C_{CH_4} = 0.2 \pm 0.3*day \ -47 \ \pm 2$, $r^2 = 0.03$, $p = 0.32$; $\delta^{2}H_{CH_4} = 0.03 \pm 0.14*day \ -96 \ \pm 11$, $r^2 = 0.005$, $p = 0.72$; $\delta^{13}C_{CO_2} = -0.05 \pm 0.16*day \ -19.9 \ \pm 1.8$, $r^2 = 0.006$, $p = 0.57$). In locations where more than one sample was taken with *in-situ* methods, the values of the samples were averaged. In total, 199 CH_4 concentrations, 192 CO_2 concentrations, 32 $\delta^{13}C_{CH_4}$ values, 26 $\delta^{2}H_{CH_4}$ values, and 60 $\delta^{13}C_{CO_2}$ values are reported in this study (Supplemental Tables 1, 2). All samples are reported with 95 % confidence intervals.

Three different modeling techniques were used to assess trace gas sources and sinks in the studied caves. Keeling plots of $\delta^{13}C_{CH_4}$, $\delta^{2}H_{CH_4}$, and $\delta^{13}C_{CO_2}$ were used to assess the possibility of a two end member mixing systems. The stable isotopic composition of CO_2 entering the caves ($\delta^{13}C_s$) was assessed through equation 1

$$\delta^{13}C_s = (\delta^{13}C_m - F_{atm} * \delta^{13}C_{atm}) (1 - F_{atm})^{-1} \quad (1)$$

where $\delta^{13}C_m$ is the $\delta^{13}C_{CO_2}$ of the sample, $\delta^{13}C_{atm}$ is the $\delta^{13}C_{CO_2}$ of the atmosphere, and F_{atm} is the fraction of atmospheric CO_2 in the CO_2 concentration of the sample (Peyraube et al., 2016). We used values of −10 ‰ for $\delta^{13}C_{atm}$ and 400 ppmv for the concentration of atmospheric CO_2.

Rayleigh distillation models were used as the theoretical basis to examine changes in the stable isotopic composition of CH_4 in cave air caused by methanotrophy or ·OH oxidation. The δ-value of an isotope system in a chemical compound of interest (e.g., CH_4) in cave air can be modeled as

$$\delta_c = (\delta_i + 1000) f^{(-\alpha + 1)} - 1000 \quad (2)$$

where δ_c is the instantaneous δ-value of a particular isotope system in cave air after partial consumption, δ_i is the initial δ-value of the isotope system in cave air, f is the fraction of the compound remaining, and α is the kinetic isotope fractionation factor (Mattey et al., 2013). α values of 1.018 and 1.1353 were used to model changes in $\delta^{13}C_{CH_4}$ and $\delta^{2}H_{CH_4}$ caused by methanotrophy (Coleman et al., 1981; Feisthauer et al., 2011). α values for changes in $\delta^{13}C_{CH_4}$ caused by methanotophy have been observed to range from 1.003 to 1.039 (Templeton et al., 2006; Feisthauer et al., 2011); 1.018 was selected based on observations of methanotrophy in soils and its similarity to the α value of 1.012 observed in St. Michael's Cave in Gibraltar (Feisthauer et al., 2011; Mattey et al., 2013). α values of 1.0039 and 1.294 were used to model changes in $\delta^{13}C_{CH_4}$ and $\delta^{2}H_{CH_4}$ values caused by ·OH oxidation (Saueressig et al., 2001). The initial stable isotopic composition of atmospheric CH_4 was modeled with a $\delta^{13}C_{CH_4} = -47.5$ ‰ (VPDB), and $\delta^{2}H_{CH_4} = -100$ ‰ (VSMOW) based on the work of Townsend-Small et al. (2012).

We examined the possibility of additional CH_4 sources entering the cave systems through forward modeling. We assumed that two different sources of microbially produced CH_4 contribute to cave air in addition to the atmosphere. We modeled CH_4 produced from acetate fermentation as S1 ($\delta^{13}C_{CH_4} = -49$ ‰ VPDB, $\delta^{2}H_{CH_4} = -325$ ‰ VSMOW) and from carbonate reduction as S2 ($\delta^{13}C_{CH_4} = -63$ ‰ VPDB, $\delta^{2}H_{CH_4} = -125$ ‰ VSMOW) respectively (Whiticar, 1999; Etiope and Sherwood Lollar, 2013). These sources were mixed with cave air both prior to and after partial theoretical methanotrophic oxidation. Methanotrophic oxidation was modeled with the aforementioned α values of 1.018 and 1.1353.

3. Results

Each of the 36 caves showed atmospheric to subatmospheric CH_4 concentrations in at least one location. Only five locations from three different caves showed elevated CH_4 concentrations relative to the atmosphere (Fig. 2, Supplemental Table 1). The CH_4 concentration in the atmosphere at study sites ranged from 1.8 ± 0.3 to 2.8 ± 0.7 ppmv. CH_4 concentrations in cave air ranged from ≤ 0.1 ± 0.1 ppmv to 5 ± 1 ppmv, and were generally observed to decrease with the distance from cave entrances (Fig. 3, Supplemental Table 1). Two thirds of the caves where three or more air measurements and distance data were recorded showed decreases in CH_4 concentration from cave entrances to interiors. For example, caves 7, 8, and 9 from Kentucky all showed progressive decreases in CH_4 concentration from about 2 ppmv at the entrance of the cave, down to zero or near zero ppmv in the more inner rooms (from 2 to 0 in caves 8 and 9 and from 1.9 to 0.3 ppmv in cave 7). Additionally, CH_4 concentrations were negatively correlated with CO_2 concentrations in cave air following an inverse power law relationship ($[CH_4] = 17.5[CO_2]^{-0.41}$, $r^2 = 0.26$) (Fig. 2). In the caves where Rn concentrations were measured, the average CO_2 concentration of cave air was correlated with the average Rn concentration of cave air ($[CO_2] = (1.42 \pm 0.09)[Rn] + 400 \pm 120$, $n = 4$, $r^2 = 0.99$, $p = 0.009$).

Values of $\delta^{13}C_{CO_2}$ in cave air ranged from −10.7 ± 0.4 to −23.81 ± 0.10 ‰. Analysis of $\delta^{13}C_{CO_2}$ values from samples with CO_2 concentrations above 600 ppmv showed that $\delta^{13}C_s$ ranging from −28 ‰ to −20 ‰ contributed to the composition of CO_2 in cave air. Pooled analysis of the CO_2 dataset shows that the average apparent source $\delta^{13}C_{CO_2}$ value is −23.3 ± 0.5 ‰ ($\delta^{13}C_{CO_2} = 4600\ [CO_2]^{-1} - 23.3 \pm 0.5$ ‰, $r^2 = 0.83$) (Fig. 4).

Values of $\delta^{13}C_{CH_4}$ and $\delta^{2}H_{CH_4}$ in cave air ranged from to −57.2 ± 0.6 to −27.1 ± 0.2 ‰ and −196 ± 10 to +2 ± 18 ‰, respectively. Keeling plots of $\delta^{13}C_{CH_4}$ did not suggest that a two end member model was an adequate fit for the system ($\delta^{13}C_{CH_4}$ vs. $[CH_4]^{-1}$: r^2 = 0.05, $\delta^{2}H_{CH_4}$ vs. $[CH_4]^{-1}$: r^2 = 0.12). Some cave air samples plotted near the theoretical relationship between $\delta^{13}C_{CH_4}$ values and CH_4 concentrations caused by methanotrophy (Fig. 5). However, many points fell below and to the left of the line representing the theoretical incomplete oxidation of atmospheric CH_4 (Figs. 5, 6). When $\delta^{2}H_{CH_4}$ and $\delta^{13}C_{CH_4}$ values were plotted against each other, many samples clustered tightly near the signature of atmospheric CH_4 (Fig. 7). Some points, like those from caves 25 and 26, plotted near the expected trend of partial atmospheric CH_4 oxidation by methanotrophy. The modeled $\delta^{13}C_{CH_4}$ and $\delta^{2}H_{CH_4}$ values of cave air overlapped with our collected samples (Figs. 5, 6, 7, Supplemental Table 3).

4. Discussion

4.1. Subsurface-Surface Atmospheric Exchange

The concentrations and stable isotopic compositions of CH_4, CO_2, and Rn in cave air overlapped and diverged from those of the atmosphere. This suggests that atmospheric and internal cave processes influenced the composition of cave air. The majority of cave air samples were depleted in CH_4 and enriched in CO_2 relative to the local atmosphere. This points to processes like *in-situ* CH_4 oxidation and diffusion of air from the epikarst to decrease CH_4 and increase CO_2 concentrations (Fig. 2). Many study locations local atmospheric CH_4 concentrations were above the globally averaged atmospheric background which may have been due to their proximity to roads or pastures with local CH_4 sources (Gioli et al., 2012; Harper et al., 2014).

The decreases in CH_4 concentration in cave air were associated with increases in cave air residence time. CH_4 concentrations were correlated with increases in the distance from a cave entrance, CO_2 concentration, Rn concentration, and decreases in $\delta^{13}C_{CO_2}$ values (Figs. 2, 3). The relationship between the distance to a cave entrance and the residence time of air in a particular cave is multivariate and we observed departures from this trend in several caves. For example, caves 13 and 15 experienced fast airflow, cave air was flowing out of the entrance of cave 26, cave 24 has multiple entrances which likely result in multiple flow paths, in cave 20 the distance scale of the measurements may have been too small to observe a decrease in CH_4 concentration, and internal CH_4 sources, which were present in cave 9, may obscure the relationship.

The concentration of Rn in cave air is known to track cave air residence time and has been observed to correlate with CO_2 concentrations. We observed correlations between cave air CO_2 and Rn concentrations. This matches other observations from the literature (Kowalczk and Froelich, 2010; Gregorič et al., 2011; as well as others). CO_2 concentrations were negatively correlated with CH_4 concentrations. This provides strong evidence that CH_4 concentrations decreased with cave air residence time. Additionally, the $\delta^{13}C_{CO_2}$ values exhibited a continuum between atmospheric values of −10 ‰ at low concentrations and decreased as CO_2 concentrations increased. The projected $\delta^{13}C_s$ values ranged from −28 to −20 ‰ with an average $\delta^{13}C_{CO_2}$ value of −23.3 ± 0.5 ‰ entering the caves. This matches the $\delta^{13}C_{CO_2}$ of soils of −24 ‰ (Amundson et al., 1998) (Fig. 4). It is possible that the observed source values that are more negative than −24 ‰ may be due to dripwater degassing or fast airflow (Spötl et al., 2005; Garcia-Anton et al., 2014). The $\delta^{13}C_s$ values that are more positive than −24 ‰ may be caused by differential abundances of C3 and C4 plants above the caves (Breecker et al., 2012). Our CO_2 data show that cave air

284 residence time increased as the CH_4 concentrations and $\delta^{13}C_{CO_2}$ values of cave air decreased, and
285 that the caves in our study are not atypical compared to other caves in the literature.

286 In some of the caves where we measured Rn concentrations, cave air flow was relatively
287 fast. The average CO_2 and Rn concentrations from these caves were relatively low (cave 33, $[CO_2]$
288 = 540 ± 20 ppmv, [Rn] = 20 ± 100 Bq m^{-3}; cave 34, $[CO_2]$ = 560 ± 30 ppmv, [Rn] = 200 ± 400
289 Bq m^{-3}). Despite the similarity to atmospheric CO_2 concentrations in these caves, average CH_4
290 concentrations were still depleted relative to the atmosphere (cave 33, $[CH_4]$ = 1.07 ± 0.06 ppmv;
291 cave 34, $[CH_4]$ = 1.34 ± 0.06 ppmv). These observations show that an *in-situ* process is removing
292 CH_4 from the cave air because subatmospheric CH_4 concentrations in cave air are still observed in
293 the absence of large increases in CO_2 concentrations as would be expected if CH_4 were only diluted
294 by the arrival of CH_4-free air into caves from soils. These observations agree with other
295 observations of fast CH_4 oxidation in caves (Fernandez-Cortes et al., 2015; Lennon et al., 2017;
296 Warring et al., 2017). Landscape scale CH_4 flux data from karst areas are needed to estimate the
297 size of the karst sink.

298

299 *4.2. Sources and Stable Isotopic Composition of Methane*

300 Our CH_4 concentration, $\delta^{13}C_{CH_4}$, and $\delta^{2}H_{CH_4}$ data from caves show that caves have sources
301 of non-atmospheric CH_4. Additional sources of CH_4 entering caves were detected by CH_4
302 concentrations above the atmospheric background in three caves, namely (i) cave 3, Indiana, (ii)
303 cave 22, Tennessee, and (iii) cave 32, New Zealand. Caves with CH_4 concentrations above the
304 atmospheric background appear to be uncommon, and understanding if there is a systematic
305 change in karst landscapes from lower order to higher order drainages awaits future work.

Peer-reviewed version available at Earth and Planetary Science Letters 2018, 485, 9-18; doi:10.1016/j.epsl.2017.12.025

306 The departures of $\delta^{13}C_{CH_4}$ and $\delta^{2}H_{CH_4}$ values from the theoretical oxidations lines of
307 atmospheric CH_4 show that caves have non-atmospheric CH_4 sources. Our data point to the
308 methanogenic sources of acetate fermentation and carbonate reduction (Fig. 7). Other studies have
309 also shown microbially produced CH_4 entering caves (Mattey et al., 2013; Webster et al., 2016).
310 Mixing between residual atmospheric CH_4 from partial methanotophic oxidation and CH_4 from
311 acetate fermentation in the soil-epikarst-cave system will generally cause a decrease in the $\delta^{13}C_{CH_4}$
312 and $\delta^{2}H_{CH_4}$ values of cave air compared to the oxidation of atmospheric CH_4, and this is supported
313 by our modeling (Figs. 5, 6). For example, caves 23, 24, and 26 all appear to be influenced by
314 acetoclastic methanogenesis.

315 CH_4 produced from carbonate reduction is inferred to enter the caves based on samples that
316 had $\delta^{2}H_{CH_4}$ values that were roughly equal to, or more positive than atmospheric values (Fig. 7).
317 The stable isotopic compositions of CH_4 from caves 5, 15, 25, and 27 can be explained by partial
318 methanotrophic consumption of CH_4 generated from carbonate reduction with the strongest source
319 signal in cave 5 (Fig. 7). CO_2 reduction is typically observed in lake sediments, but has been
320 observed in oxidizing environments such as biological soil crusts in deserts after rain events (Angel
321 et al., 2011). We hypothesize that karst environments, which are less oxidizing, exhibit similar
322 behavior. Our data show that carbonate reduction and acetate fermentation can occur in similar
323 environments over large spatial scales and are not limited to aquatic and arctic environments.

324 Sites of methanogenesis in or near the studied cave systems may include waterlogged soils
325 above caves, cave soils themselves, and the epikarst. It is possible that after rain events anoxic
326 micro niches occur in soil, or the epikarst and the generated CH_4 is dissolved and later introduced
327 into caves with drip waters. We confirmed that dissolved CH_4 outgasses in drip water of cave 32,
328 which was situated underneath a wetland, by placing our CH_4 detecting probe near the water and

329 measuring increased CH_4 concentrations in its vicinity. We confirmed that *in-situ* CH_4 production
330 can take place in locally anoxic environments within caves by measuring CH_4 concentrations close
331 to a bat guano deposit in cave 25, Tennessee (site 4h; average CH_4 concentration = 0.3 ± 0.5 ppmv).
332 Time series measurements near the large bat guano deposit showed that CH_4 concentrations
333 oscillated between 0.5 ppmv and 0.1 ppmv over the course of seconds, presumably in response to
334 episodic migration of CH_4 bubbles through the moist guano (similar oscillations in ammonia, NH_3,
335 were also observed). Additionally, we observed circumstantial evidence for local *in-situ* CH_4
336 production in cave 3 because measured CH_4 concentrations upstream of a restroom in the cave
337 were low, while measured CH_4 concentrations downstream of the restroom were enhanced. Our
338 data show that caves are capable of expressing elevated CH_4 concentrations due to *in-situ* CH_4
339 production when accumulations of organic matter, such as guano or plant material, foster
340 methanogenesis or when dissolved CH_4 from waters outgasses into cave air.

341 We observed minor amounts of thermogenic CH_4 entering in at least one cave. Locally
342 elevated CH_4 concentrations in cave 9 (Mammoth Cave, Kentucky) were associated with a known
343 hydrocarbon seep that is also transporting sulfide (Olson, 2013). Elevated CH_4 concentrations,
344 thought to derive from thermogenic CH_4, have also been observed at sulfidic springs in *Cueva de*
345 *Villa Luz* (Webster et al., 2017). Some $\delta^{13}C_{CH_4}$ and $\delta^{2}H_{CH_4}$ values in cave air, i.e. two of the samples
346 from cave 24, are compatible with thermogenic CH_4 isotopic signatures (e.g., Schoell, 1988;
347 Etiope et al., 2009; Fig. 7). It cannot be excluded that small fluxes of CH_4 from shales or
348 hydrocarbon deposits underlying the limestone are entering caves through natural fractures, but
349 our present isotope data cannot confirm this source for cave 24. The Antes and Utica shales, which
350 contain hydrocarbon gases, are stratigraphically below cave 24 (Coleman et al., 2014), and
351 geologic faults and joints, which are often aligned with caves, may serve as conduits for the flow

of hydrocarbons (Powell, 1969). A confirmation of hydrocarbons entering from deep sources may be obtained through measurements of 'radiocarbon-dead' CO_2, Rn, and ethane.

4.3. Methane Oxidation Mechanisms

The combination of $\delta^{13}C_{CH_4}$ and $\delta^{2}H_{CH_4}$ values allow for inferences to be made about the CH_4 oxidizing reactions in karst environments. We distinguish between two scenarios with distinct sets of assumptions. Many isotopic compositions of CH_4 in this study cannot be accounted for in a first scenario in which we assume that (i) CH_4 enters the caves from the atmosphere, through acetate fermentation, and through carbonate reduction, and that (ii) CH_4 is removed from cave air through reactions involving the ·OH. Conversely, in a second scenario, if it is assumed that (i) sources of CH_4 in cave air include the atmosphere, acetate fermentation, and carbonate reduction, and that (ii) CH_4 is removed from cave air by methanotrophy, all of the points fall within the plausibility envelope of the model, suggesting that methanotrophy is the mechanism responsible for removing CH_4 from cave air (Fig. 7). Consideration of an additional source of thermogenic CH_4 (natural gas) from deep geologic sources enlarges the plausibility fields of both prior scenarios to encompass all of the data. Furthermore, the modeled isotopic composition of cave air, which has the same assumptions as the second scenario, overlays comparably with our data set.

Our $\delta^{13}C_{CH_4}$ and $\delta^{2}H_{CH_4}$ data also agree with observations of $\delta^{13}C_{CH_4}$ and $\delta^{2}H_{CH_4}$ from a cave in Indiana where it appeared that CH_4 from both acetate fermentation and carbonate reduction influenced cave air geochemistry (Webster et al., 2016). Additionally, our data resemble an arctic system characterized by acetoclastic and hydrogenotrophic CH_4 sources and methanotrophy (McCalley et al., 2014). Our isotopic evidence for *in-situ* microbial CH_4 oxidation in caves is

corroborated by recent results from *in-situ* mesocosm experiments in Vietnam where cave rocks with live microorganisms were shown to consume CH_4 even in cases where surface soils were very thin to non-existent (Lennon et al., 2017; Nguyễn-Thuỳ et al., 2017).

5. Conclusions

1) CH_4 consumption is the dominant process in karst landscapes. Subterranean karst air generally shows subatmospheric CH_4 concentrations. CH_4 and CO_2 concentrations were negatively correlated in cave air showing that as the residence time of cave air increases the CH_4 concentration of cave air decreases. CH_4 concentrations decreased faster than increases in CO_2 concentration in cave air demonstrating that an *in-situ* process is responsible for the removal of CH_4 from cave air.

2) The stable isotopic composition of CH_4 in studied caves suggests that CH_4 is being oxidized by microbial methanotrophy. This evidence adds to reports that methanotrophy is the mechanism by which CH_4 is rapidly removed in cave air (Mattey et al., 2013; McDonough et al., 2016; Webster et al., 2016; Lennon et al., 2017, Waring et al., 2017). The observations of sub-atmospheric CH_4 concentrations in cave air from this and other studies show that karst is behaving as a global CH_4 sink.

3) The stable isotopic composition of CH_4 in the studied caves suggests that, in addition to atmospheric CH_4, at least two additional CH_4 sources are present in some caves. We suggest that the sources include CH_4 produced from acetate fermentation and from CO_2 reduction. These data corroborate recent findings of partially oxidized CH_4 entering cave air from acetate fermentation and CO_2 reduction in Indiana (Webster et al., 2016). These

observations of CH_4 production by acetate fermentation and carbonate reduction suggest that both processes happen over a wide scale in the environment.

Acknowledgements

This material is based upon work supported by the U.S. Department of Energy, Office of Science, Office of Basic Energy Sciences, Chemical Sciences, Geosciences, and Biosciences Division under Award Number DE-SC0006978. This study was partially funded by NASA ASTEP (Award # NNX11AJ01G) and a National Speleological Society research grant. We thank J. Forsythe of Lost River Cave (cave 7) and R. S. Toomey III of Mammoth Cave National Park for granting access. Members of the Bloomington Indiana Grotto facilitated access to caves in Indiana. The Richard Blenz Nature Conservancy permitted access to cave 35. We thank M. Lefticariu and J. Hayden-Moore of Little Egypt Grotto in Carbondale, Illinois for providing assistance and access to gas sampling in cave 36 (SE Missouri). T.V. Royer in SPEA at Indiana University made analytical gas chromatography available. We are grateful for constructive comments from H.M. Stoll and three anonymous reviewers.

References

Amundson, R., Stern, L., Baisden, T., Wang, Y., 1998. The isotopic composition of soil and soil-respired CO_2. Geoderma 82, 83–114. http://dx.doi.org/10.1016/S0016-7061(97)00098-0

Angel, R., Matthies D., Conrad, R., 2011. Activation of methanogenesis in arid biological soil crusts despite the presence of oxygen. PLoS ONE 6(5), e20453. http://dx.doi.org/10.1371/journal.pone.0020453

418 Batiot-Guilhe, C., Seidel, J.-L., Jourde, H., Hébrard, O., Bailly-Comte, V., 2007. Seasonal
419 variations of CO_2 and ^{222}Rn in a Mediterranean sinkhole – sping (Causse d'Aumelas, SE
420 France). International Journal of Speleology 36(1), 51-56.

421 Breecker, D.O., Payne, A.E., Quade, J., Banner, J.L., Ball, C.E., Meyer, K.W., Cowan, B.D., 2012.
422 The sources and sinks of CO_2 in caves under mixed woodland and grassland vegetation.
423 Geochimica et Cosmochimica Acta 96, 230-246.
424 http://dx.doi.org/10.1016/j.gca.2012.08.023

425 Ciais, P., Sabine, C., Bala, G., Bopp, L., Brovkin, V., Canadell, J., Chhabra, A., DeFries, R.,
426 Galloway, J., Heimann, M., Jones, C., Le Quéré, C., Myneni, R.B., Piao, S., Thornton, P.,
427 2013. Carbon and other biogeochemical cycles. *In* (Stocker, T.F., Qin, D., Plattner, G.-K.,
428 Tignor, M., Allen, S.K., Boschung, A., Nauels, A., Xia, Y., Bex, V., Midgley, P.M., eds.)
429 Climate Change 2013: The Physical Science Basis. Contribution to Working Group I to
430 the Fifth Assessment Report of the Intergovernmental Panel on Climate Change.
431 Cambridge University Press, Cambridge, United Kingdom and New York, NY, USA.

432 Coleman D.D., Risatti J.B., Schoell M., 1981. Fractionation of carbon and hydrogen isotopes by
433 methane-oxidizing bacteria. Geochimica et Cosmochimica Acta 45(7), 1033-1037.
434 http://dx.doi.org/10.1016/0016-7037(81)90129-0

435 Coleman, J.L., Jr., Ryder, R.T., Milici, R.C., Brown, S., 2014. Overview of the potential and
436 identified petroleum source rocks of the Appalachian Basin, Eastern United States. *In*
437 (Ruppert, L.F., Ryder, R.T., eds.) Coal and Petroleum Resources in the Appalachian basin;
438 Distribution, Geologic Framework, and Geochemical Character: U.S. Geological Survey
439 Professional Paper 1708, http://dx.doi.org/10.3133/pp1708G.13

440 Cunningham, K.I., LaRock, E.J., 1991. Recognition of microclimate zones through radon
441 mapping, Lecheguilla Cave, Carlsbad Caverns National Park, New Mexico. Health Physics
442 61(4), 493-500.

443 Dlugokencky, E.J., Houweling, S., Bruhwiler, L., Masarie, K.A., Lang, P.M., Miller, J.B., Tans,
444 P.P., 2003. Atmospheric methane levels off: Temporary pause or a new steady state?
445 Geophysical Research Letters 30 (1992), http://dx.doi.org/10.1029/2003GL018126

446 Dlugokencky, E.J., Nisbet, E.G., Fisher, R., Lowry, D., 2011. Global atmospheric methane: budget
447 changes, and dangers. Phil. Trans. R. Soc. A 369, 2058-2072.
448 http://dx.doi.org/10.1098/rsta.2010.0341

449 Etiope G., Feyzullayev A., Baciu C.L., 2009. Terrestrial methane seeps and mud volcanoes: a
450 global perspective of gas origin. Marine and Petroleum Geology 26, 333-344.
451 http://dx.doi.org/10.1016/j.marpetgeo.2008.03.001

452 Feisthauer, S., Vogt, C., Modrzynski, J., Szlenkier, M., Krüger, M., Siegert, M., Richnow, H.-H.,
453 2011. Different types of methane monooxygenases produce similar carbon and hydrogen
454 isotope fraction patterns during methane oxidation. Geochimica et Cosmochimica Acta
455 75(5), 1173-1184. http://dx.doi.org/10.1016/j.gca.2010.12.006

456 Fernandez-Cortes, A., Cuezva, S., Alvarez-Gallego, M., Garcia-Anton, E., Pla C., Benavente, D.,
457 Jurado V., Saiz-Jimenez, C., Sanchez-Moral, S., 2015. Subterranean atmospheres may act
458 as daily methane sinks. Nature Communications 6(7003).
459 http://dx.doi.org/10.1038/ncomms8003

460 Garcia-Anton, E., Cuezva, S., Fernandez-Cortes, A., Benavente, D., Sanchez-Moral, S., 2014.
461 Main drivers of diffusive and advective processes of CO_2-gas exchange between a shallow

462 vadose zone and the atmosphere. International Journal of Greenhouse Gas Control 21, 113-
463 129. http://dx.doi.org/10.1016/j.ijggc.2013.12.006

464 Ford, D., Williams, P., 2007. Karst Hydrogeology and Geomorphology. John Wiley & Sons Ltd,
465 England.

466 Gioli, B., Toscano, P., Lugato, E., Matese, A., Migilietta, F., Zaldei, A., Vaccari, F.P., 2012.
467 Methane and carbon dioxide fluxes and source partitioning in urban areas: The case study
468 of Florence, Italy. Environmental Pollution 164, 125-131.
469 http://dx.doi.org/10.1016/j.envpol.2012.01.019

470 Gregorič, A., Zidanšek, A., Vaupotič, J., 2011. Dependence of radon levels in Postojna Cave on
471 outside air temperature. Natural Hazards and Earth System Sciences 11, 1523-1528.
472 http://dx.doi.org/ 10.5194/nhess-11-1523-2011

473 Gregorič, A., Vaupotič, J., Šebela, S., 2014. The role of cave ventilation in governing cave air
474 temperature and radon levels (Postojna Cave, Slovenia). International Journal of
475 Climatology 34(5), 1488-1500. http://dx.doi.org/10.1002/joc.3778

476 Harper, L.A., Weaver, K.H., De Visscher, A., 2014. Dinitrogen and methane gas production during
477 the anaerobic/anoxic decomposition of animal manure. Nutrient Cycling in
478 Agroecosystems 100(1), 53-64. http://dx.doi.org/10.1007/s10705-014-9626-9

479 Hutchens, E., Radajewski, S., Dumont, M.G., McDonald, I.R., Murrell, J.C., 2004. Analysis of
480 methanotrophic bacteria in Movile Cave by stable isotope probing. Environmental
481 Microbiology 6(2), 111-120. http://dx.doi.org/10.1046/j.1462-2920.2003.00543.x

482 Jones, D.S., Albrecht, H.L., Dawson, K.S., Schaperdoth, I., Freeman, K.H., Pi, Y., Pearson, A.,
483 Macalady, J.L., 2012. Community genomic analysis of an extremely acidophilic sulfur
484 oxidizing biofilm. The ISME Journal 6, 158-170. http://dx.doi.org/10.1038/ismej.2011.75

485 Kirschke, S., Bousquet, P., Ciais, P., Saunois, M., Canadell, J.G., Dlugokencky, E.J., Bergamaschi,
486 P., Bergmann, D., Blake, D.R., Bruhwiler, L., Cameron-Smith, P., Castaldi, S., Chevallier,
487 F., Feng, L., Fraser, A., Heimann, M., Hodson, E.L., Houweling, S., Josse, B., Fraser, P.J.,
488 Krummel, P.B., Lamarque, J.-F., Langenfelds, R.L., Le Quéré, C., Naik, V., O'Doherty,
489 S., Palmer, P.I., Pison, I., Plummer, D., Poulter, B., Prinn, R.G., Rigby, M., Ringeval, B.,
490 Santini, M., Schmidt, M., Schindell, D.T., Simpson, I.J., Spahni, R., Steele, L.P., Strode,
491 S.A., Sudo, K., Szopa, S., van der Werf, G.R., Voulgarakis, A., van Weele, M., Weiss,
492 R.F., Williams, J.E., Zeng, G., 2014. Three decades of global methane sources and sinks.
493 Nature Geoscience 6, 812-8123.

494 Keeling, R.F., Piper, S.C., Bollenbacher, A.F., Walker, S.J., 2010. Monthly atmospheric $^{13}C/^{12}C$
495 isotopic ratios for 11 SIO stations. *In* Trends: A Compendium of Data on Global Change.
496 Carbon Dioxide Information Analysis Center, Oak Ridge National Laboratory, U.S.
497 Department of Energy, Oak Ridge, Tenn., U.S.A.

498 Kowalczk, A.J., Froelich, P.N., 2010. Cave air ventilation and CO_2 outgassing by radon-222
499 monitoring: How fast do caves breathe? Earth and Planetary Science Letters 289, 209-219.
500 http://dx.doi.org/10.1016/j.epsl.2009.11.010

501 Lennon, J.T., Nguyễn-Thùy, D., Phạm, T.M., Drobniak, A., Tạ, P.H., Phạm, N.Đ., Streil, T.,
502 Webster, K.D., Schimmelmann, A., 2017. Microbial contributions to subterranean methane
503 sinks. Geobiology 15(2), 254-258. http://dx.doi.org/10.1111/gbi.12214

504 Mattey, D.P., Fairchild, I.J., Atkinson, T.C., Latin, J.-P., Ainsworth, M., Durell, R., 2010. Seasonal
505 microclimate control of calcite fabrics, stable isotopes and trace elements in modern
506 speleothem from St. Michaels Cave, Gibraltar. *In* (Pedley, H.M., Rogerson, M. eds.) Tufas
507 and Speleothems: Unravelling the Microbial and Physical Controls: Geological Society,
508 London, Special Publications 336, 323-344. http://dx.doi.org/10.1144/SP336.17

509 Mattey, D.P., Fisher, R., Atkinson, T.C., Latin, J.-P., Durrell, R., Ainsworth, M., Lowry, D.,
510 Fairchild, I.J., 2013. Methane in underground air in Gibraltar karst. Earth and Planetary
511 Science Letters 374, 71-80. http://dx.doi.org/10.1016/j.epsl.2013.05.011

512 McCalley, C.K., Woodcroft, B.J., Hodgkins, S.B., Wehr, R.A., Kim, E.-H., Mondav, R., Crill,
513 P.M., Chanton, J.P., Rich, V.I., Tyson, G.W., Saleska, S.R., 2014. Methane dynamics
514 regulated by microbial community response to permafrost thaw. Nature 514, 478-481.
515 http://dx.doi.org/10.1038/nature13798

516 McDonough, L.K., Iverach, C.P., Beckman, S., Manfield, M., Rau, G.C., Baker, A., Kelly, B.F.J.,
517 2016. Spatial variability of cave-air carbon dioxide and methane concentrations and
518 isotopic compositions in a semi-arid karst environment. Environmental Earth Sciences
519 75(700), http://dx.doi.org/10.1007/s12665-016-5497-5

520 Miller, J.B., Mack, K.A., Dissly, R., White, J.W.C., Dlugokencky, E.J., Tans, P.P., 2002.
521 Development of analytical methods and measurements of $^{13}C/^{12}C$ in atmospheric CH_4 from
522 the NOAA Climate Monitoring and Diagnostics Laboratory Global Air Sampling Network.

523 Journal of Geophysical Research: Atmospheres 107(D13), ACH 11-1-ACH 11-15.
524 http://dx.doi.org/10.1029/2001JD000630

525 Nisbet, E.G., Dlugokencky, E.J., Manning, M.R., Lowry, D., Fisher, R.E., France, J.L., Michel,
526 M.E., Miller, J.B., White, W.J.C., Vaughn, B., Bousquet, P., Pyle, J.A., Warwick, N.J.,
527 Cain, M., Brownlow, R., Zazzeri, G., Lanoisellé, M., Manning, A.C., Gloor, E., Worthy,
528 D.E.J., Brunke, E.-G., Labuschagne, C., Wolff, E.W., Ganesan, A.L., 2016. Rising
529 atmospheric methane: 2007-2014 growth and isotopic shift. Global Biogeochemical Cycles
530 30, 1356-1370. http:///dx.doi.org/10.1002/2016GB005406

531 Nguyễn-Thuỳ, D., Schimmelmann, A., Nguyễn-Văn, H., Drobniak, A., Lennon, J.T., Tạ, P.H.,
532 Nguyễn, N.T.Á., (2017). Subterranean microbial oxidation of atmospheric methane in
533 cavernous tropical karst. *Chemical Geology*.
534 https://doi.org/10.1016/j.chemgeo.2017.06.014

535 Olson, R., 2013. Potential effects of hydrogen sulfide and hydrocarbon seeps on Mammoth Cave
536 ecosystems. Mammoth Cave Research Symposia. Paper 28.
537 http://digitalcommons.wku.edu/mc_reserch_symp/10th_Research_Symposium_2013/Res
538 earch_Posters/28

539 Palmer, A.N., 1991. Origin and morphology of limestone caves. Geological Society of America
540 Bulletin 103(1), 1-21. http://dx.doi.org/10.1130/0016-
541 7606(1991)103<0001:OAMOLC>2.3.CO;2

542 Peyraube, N., Lastennet, R., Denis, A., Malaurent, P., 2013. Estimation of epikarst air P_{CO_2} using
543 measurements of water $\delta^{13}C_{TDIC}$, cave air P_{CO_2} and $\delta^{13}C_{CO_2}$. Geochimica et Cosmochimica
544 Acta 118, 1-17. http://dx.doi.org/10.1016/j.gca.2013.03.046

545 Peyraube, N., Lastennet, R., Villanueva, J.D., Houillon, N., Malaurent, P., Denis, A., 2016. Effect
546 of diurnal and seasonal temperature variation on Cussac cave ventilation using CO_2
547 assessment. Theoretical and Applied Climatology, http://dx.doi.org/10.1007/s00704-016-
548 1824-8

549 Powell, R.L. 1969. Base level, and climatic controls of karst groundwater zones in South-Central
550 Indiana. Indiana Academy of Science, 281-291.

551 Sarbu, S.M., Kane, T.C., Kinkle, B.K., 1996. A chemoautotrophically based cave ecosystem.
552 Science 272(5270), 1953-1955. http://dx.doi.org/10.1126/science.272.5270.1953

553 Saueressig, G., Crowley, J.N., Bergamaschi, P., Brühl, C., Brennikmeijer, C.A.M., Fischer, H.,
554 2001. Carbon 13 and D kinetic isotope effects in the reactions of CH4 with $O(^1D)$ and OH:
555 New laboratory measurements and their implications for the isotopic composition of
556 stratospheric methane. Journal of Geophysical Research 106 (D19), 23127–23138.
557 http://dx.doi.org/10.1029/2000JD000120

558 Schoell, M., 1988. Multiple origins of methane in the Earth, *in* Schoell, M. ed. Origins of Methane
559 in the Earth. Chemical Geology 71, 1-10. http://dx.doi.org/10.1016/0009-2541(88)90101-
560 5

561 Spötl, C., Fairchild, I.J., Tooth, A.F., 2005. Cave air control on dripwater geochemistry, Obir
562 Caves (Austria): Implications for speleothem deposition in dynamically ventilated caves.
563 Geochimica et Cosmochimica Acta 69(10), 2451-2468.
564 http://dx.doi.org/10.1016/j.gca.2004.12.009

565 Sussman, R., Forster, F., Rettinger, M., Bousquet, P., 2012. Renewed methane increase for five
566 years (2007-2011) observed by solar FTIR spectrometry. Atmospheric Chemistry and
567 Physics 12, 4885-4891. http://dx.doi.org/10.5194/acp-12-4885-2012

568 Templeton, A., Chu, K.-H., Alvarez-Cohen, L., Conrad, M.E., 2006. Variable carbon isotope
569 fractionation expressed by aerobic CH_4-oxidizing bacteria. Geochimica et Cosmochimica
570 Acta 70(7), 1739-1752. http://dx.doi.org/10.1016/j.gca.2005.12.002

571 Townsend-Small, A., Tyler, S.C., Pataki, D.E., Xu, X., Christensen, L.E., 2012. Isotopic
572 measurements of atmospheric methane in Los Angeles, California, USA: Influence of
573 "fugitive" fossil fuel emissions. Journal of Geophysical Research 117(D07308).
574 http://dx.doi.org/10.1029/2011JD016826

575 Tu, K.P., Brooks, P.D., Dawson, T.E., 2001. Using septum-capped vials with continuous-flow
576 isotope ratio mass spectrometric analysis of atmospheric CO_2 for Keeling plot applications.
577 Rapid Communications in Mass Spectrometry 15(12), 952-956.
578 http://dx.doi.org/10.1002/rcm.320

579 Waring, C.L., Hankin, S.L., Griffith, D.W.T., Kertesz, M.A., Kobylski, V., Wilson, N.L.,
580 Coleman, N.V., Kettlewell, G., Zlot, R., Bosse, M., Bell, G., 2017. Scientific Reports
581 7(8314). http://dx.doi.org/10.1038/s41598-017-07769-6

582 Weary, D.J., Doctor, D.H., 2014. Karst in the United States: A digital map compilation and
583 database: U.S. Geological Survey Open-File Report 2014–1156.
584 http://dx.doi.org/10.3133/ofr20141156

585 Webster, K.D., Mirza, A., Deli, J.M., Sauer, P.E., Schimmelmann, A., 2016. Consumption of
586 atmospheric methane in a limestone cave in Indiana, USA. Chemical Geology 443, 1-9.
587 http://dx.doi.org/10.1016/j.chemgeo.2016.09.020

588 Webster, K.D., Rosales Lagarde, L., Sauer, P.E., Schimmelmann, A., Lennon, J.T., Boston, P.J.,
589 2017. Isotopic evidence for the migration of thermogenic methane into a sulfidic cave,
590 Cueva de Villa Luz, Tabasco, Mexico. Journal of Cave and Karst Studies 79(1), 24-34.
591 https://caves.org/pub/journal/PDF/V79/cave-79-01-24.pdf.

592 Whiticar, M.J., 1999. Carbon and hydrogen isotope systematics of bacterial formation and
593 oxidation of methane. Chemical Geology 161, 291-314. http://dx.doi.org/10.1016/S0009-
594 2541(99)00092-3

595

Preprints (www.preprints.org) | NOT PEER-REVIEWED | Posted: 5 December 2017 doi:10.20944/preprints201708.0009.v3

Peer-reviewed version available at Earth and Planetary Science Letters 2018, 485, 9-18; doi:10.1016/j.epsl.2017.12.025

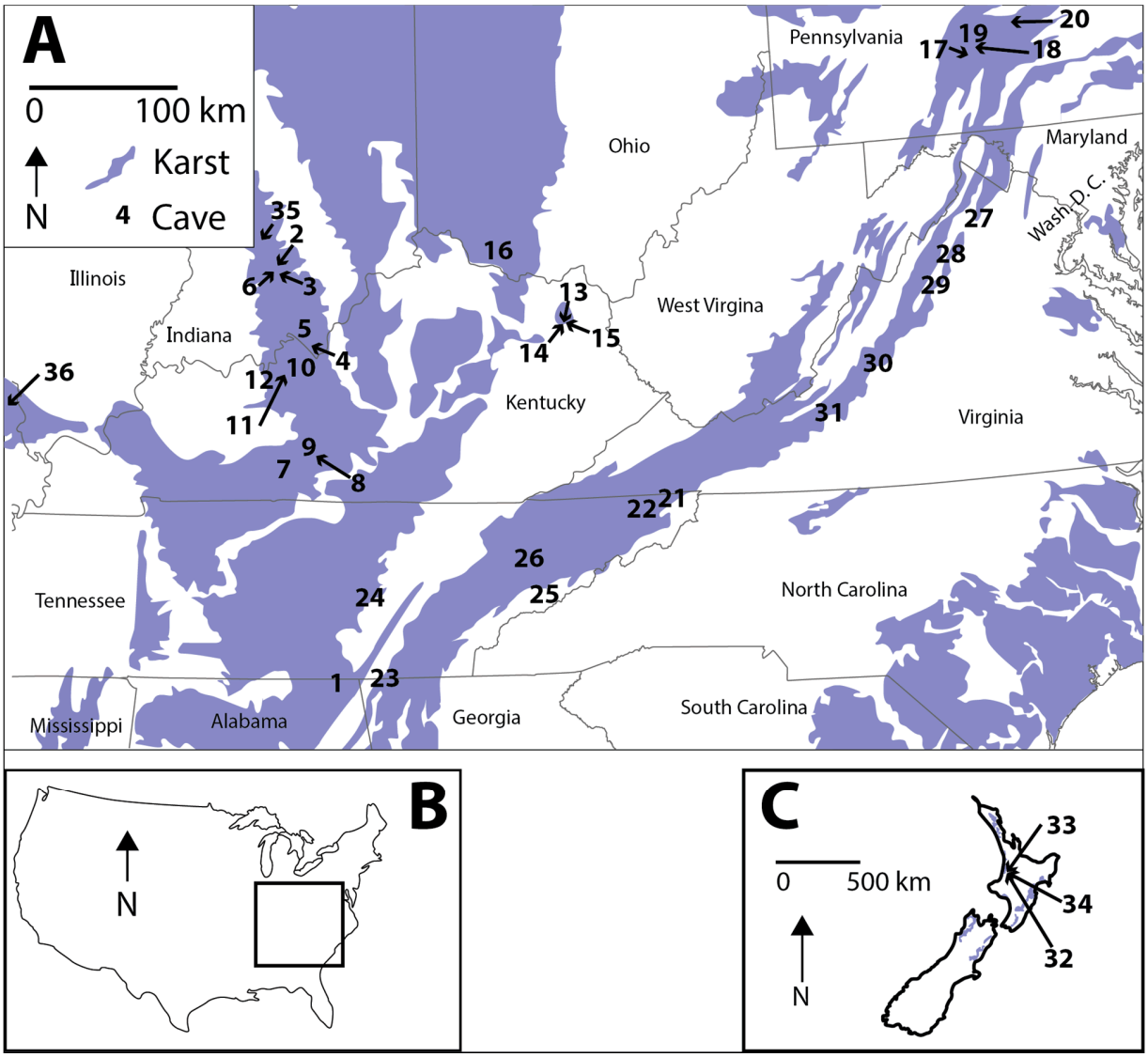

Figure 1. (A) Locations of the U.S. study caves in their regional context and (B) within the contiguous USA. (C) The location of the New Zealand caves. Karst land cover data were obtained from Weary and Doctor (2014) and Ford and Williams (2007).

Preprints (www.preprints.org) | NOT PEER-REVIEWED | Posted: 5 December 2017 doi:10.20944/preprints201708.0009.v3

Peer-reviewed version available at Earth and Planetary Science Letters 2018, 485, 9-18; doi:10.1016/j.epsl.2017.12.025

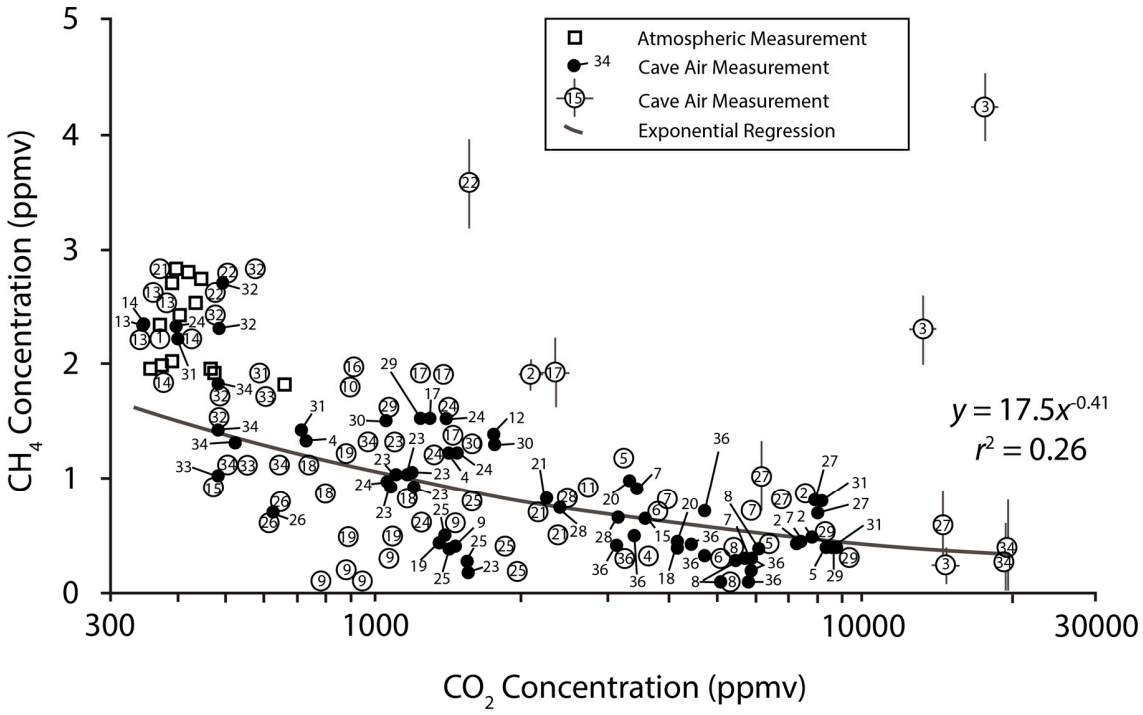

601

602 **Figure 2.** CH_4 concentrations *versus* CO_2 concentrations in studied caves. The majority of samples
603 appear to follow an inverse power law relationship with CH_4 concentrations being inversely related
604 to CO_2 concentrations (with points from caves 3 and 22 removed from the overall trend). Numbers
605 represent individual caves. For clarity, some points are shown as black dots with a line pointing to
606 the cave number of the sample. Some error bars were omitted from the figure for clarity. Data
607 associated with error bars are also representative for typical errors of data where no bars are shown.

608

Preprints (www.preprints.org) | NOT PEER-REVIEWED | Posted: 5 December 2017 doi:10.20944/preprints201708.0009.v3

Peer-reviewed version available at Earth and Planetary Science Letters 2018, 485, 9-18; doi:10.1016/j.epsl.2017.12.025

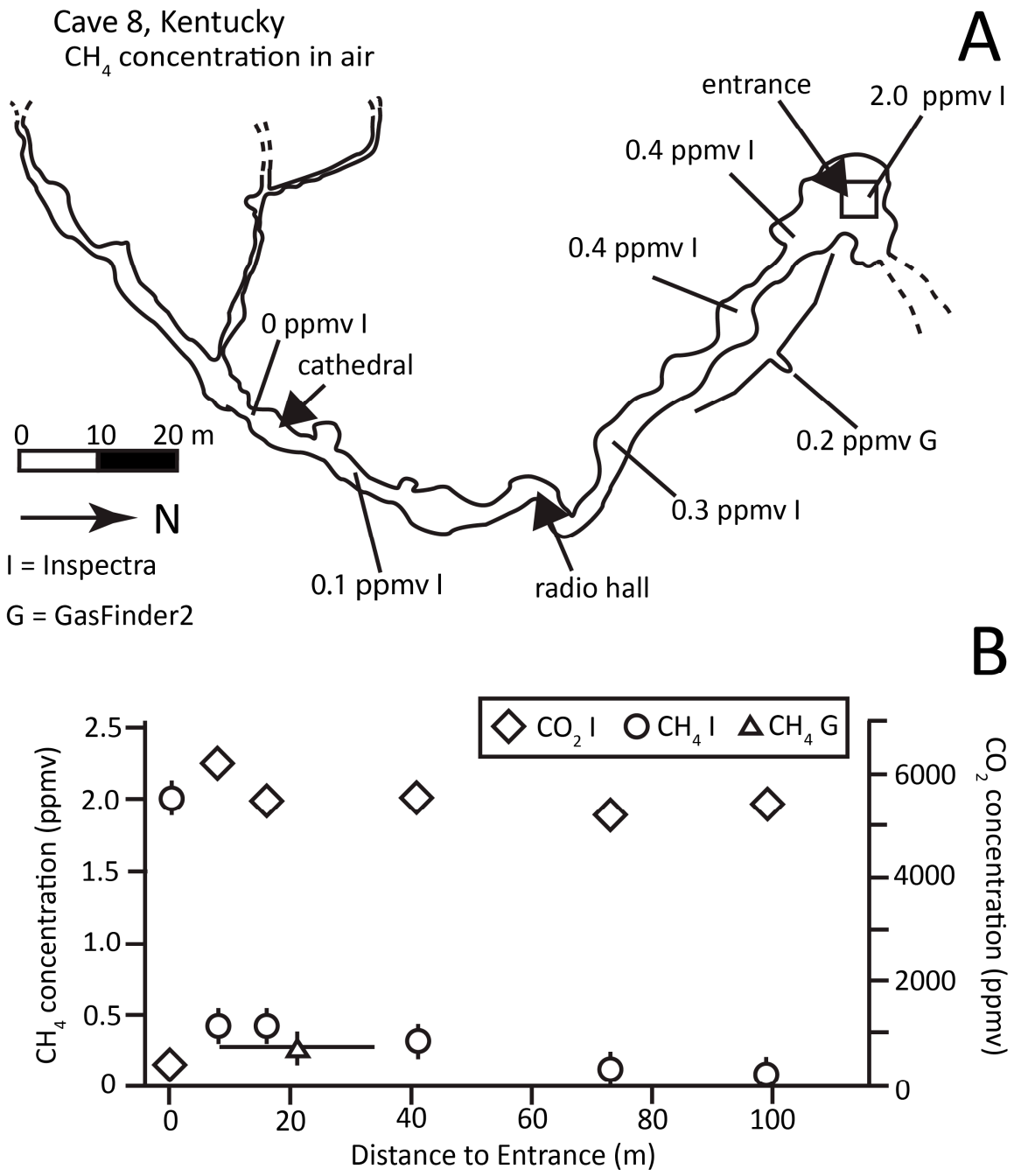

609

610 **Figure 3.** The spatial variation of CH_4 mole faction in the air of cave 8, Kentucky sampled on May

611 6, 2012. (A) CH_4 concentration dropped sharply down to 0.4 ppmv along a narrow path after the

612 first large room, a few tens of meter from the entrance. CH_4 gradually decreased over roughly 100

613 m down to 0 ppmv in the Cathedral room, (B) while CO_2 exhibited relatively constant
614 concentrations in cave air.
615

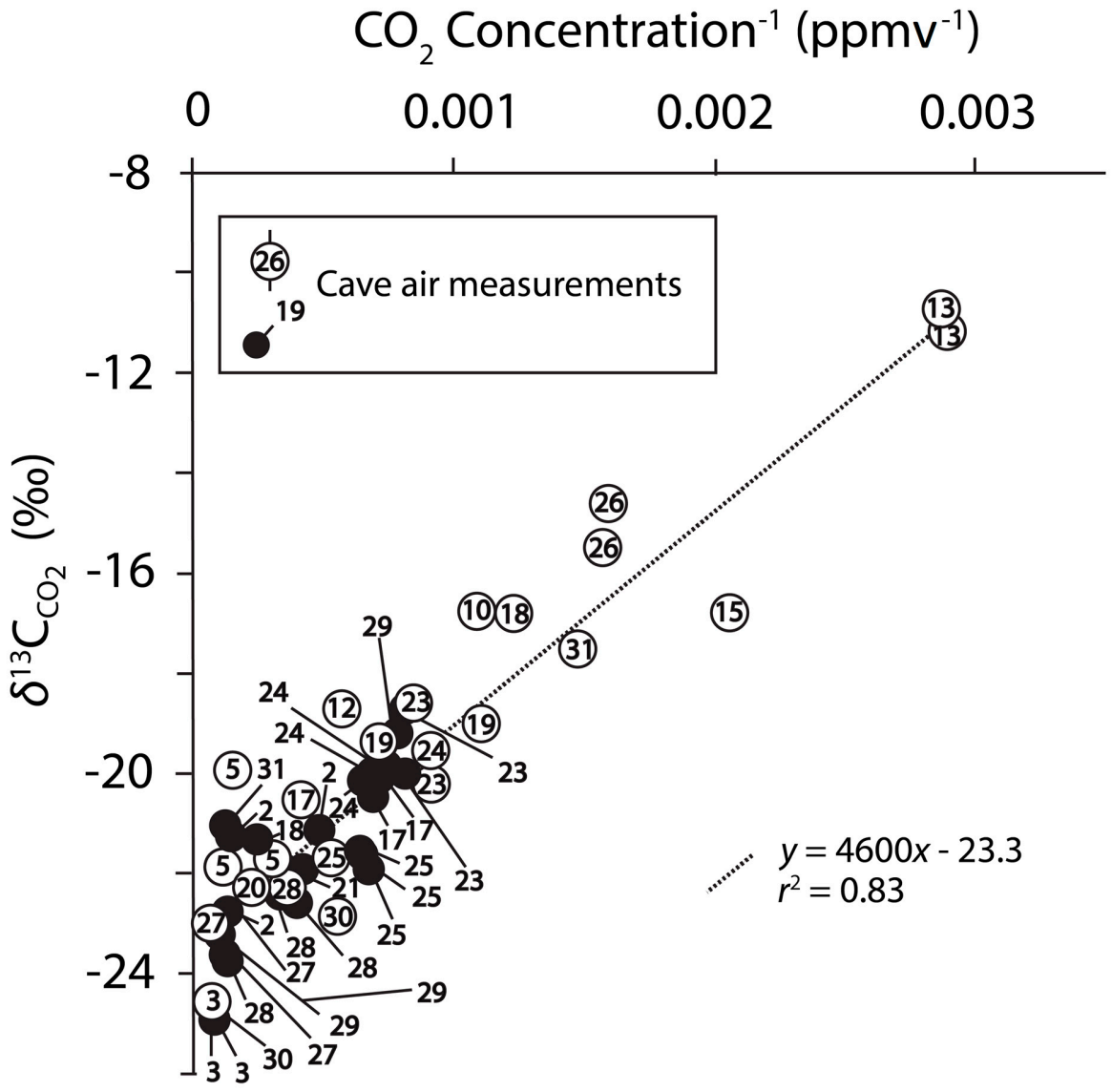

616

617 **Figure 4.** A Keeling plot of $\delta^{13}C_{CO_2}$ *versus* inverse CO_2 concentration in cave air samples. The
618 data show that atmospheric CO_2 is mixing with apparent isotopic endmembers between −33 and
619 −20.4 ‰. A regression analysis of the entire data set shows that the average $\delta^{13}C_{CO_2}$ value entering

the caves is −23.3 ± 0.5 ‰. Numbers represent individual caves. For clarity, some points are shown as black dots with a line pointing to the cave number of the sample, nor are error bars included.

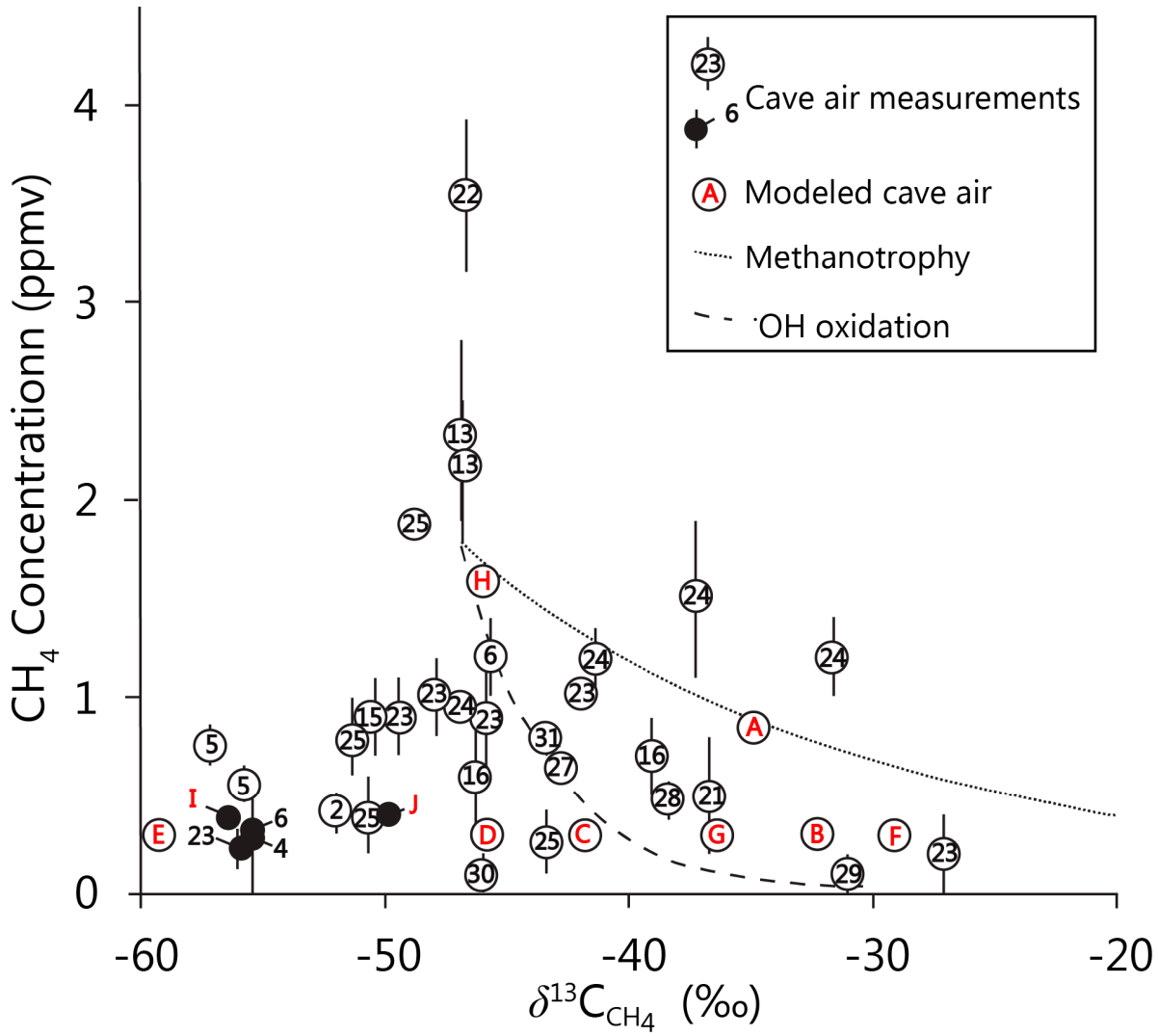

Figure 5. Relationship between CH_4 concentration and $\delta^{13}C_{CH_4}$ in cave air. Some samples plot along the expected relationship between CH_4 concentration and $\delta^{13}C_{CH_4}$ caused either by methanotrophy modeled with an α value of 1.018, or by oxidation with ·OH modeled with an α

627 value of 1.0039. Other samples plot below and to the left of the theoretical shifts of the oxidation
628 trends. Numbers represent individual caves. Note that modeled cave air, represented by letters,
629 also plots left of theoretical methanotrophic oxidation. For clarity, some points are shown as black
630 dots with a line pointing to the cave number of the sample. If error bars are not visible, they are
631 smaller than the data points.

632

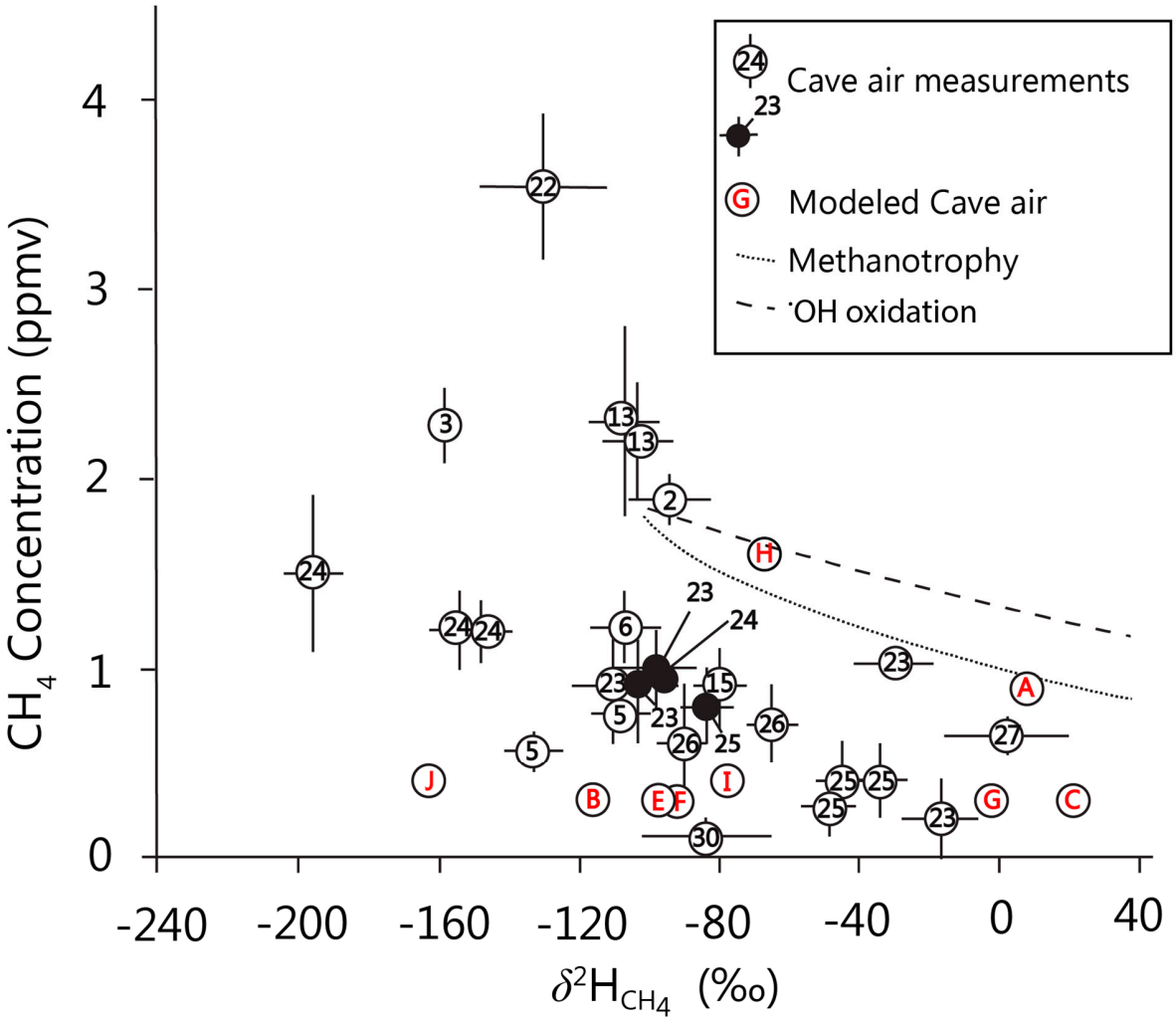

633

634 **Figure 6.** Relationship between methane concentration and $\delta^2H_{CH_4}$ in cave air. Some samples plot
635 along the expected relationship between CH_4 concentration and $\delta^2H_{CH_4}$ caused by methanotrophy
636 modeled with an α. value of 1.1353, or by oxidation with ·OH modeled with an α.value 1.294.
637 Other samples plot below and to the left of the shift caused by methanotrophy. Numbers represent
638 individual caves. Note that modeled cave air, represented by letters, generally plots left of the
639 theoretical oxidation lines. For clarity, some points are shown as black dots with a line pointing to
640 the number of the cave the sample is from. If error bars are not visible, they are smaller than the
641 data points.

642

Preprints (www.preprints.org) | NOT PEER-REVIEWED | Posted: 5 December 2017 doi:10.20944/preprints201708.0009.v3

Peer-reviewed version available at Earth and Planetary Science Letters 2018, 485, 9-18; doi:10.1016/j.epsl.2017.12.025

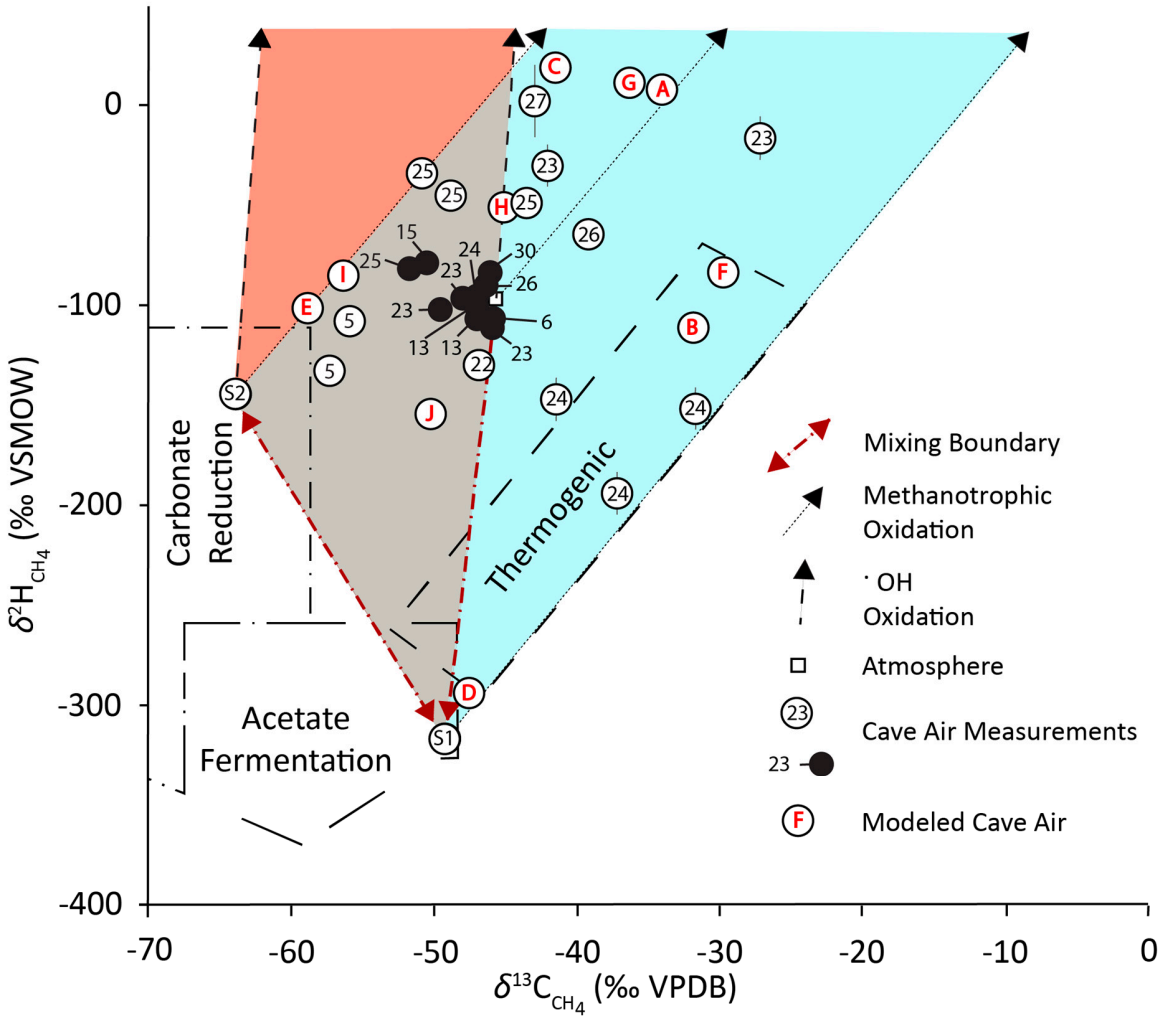

643

644 **Figure 7.** Stable isotopic composition of CH_4 in cave air samples plotted in $\delta^2H_{CH_4}$ *versus* $\delta^{13}C_{CH_4}$

645 space. CH_4 generated by carbonate reduction, acetate fermentation, and thermogenesis are plotted

646 within labeled fields (Whiticar, 1999). We model inputs from the atmosphere as (−47.5 ‰, −100

647 ‰, □), acetate fermentation as (−49 ‰, −325 ‰, S1), and carbonate reduction as (−63 ‰, −125

648 ‰, S2). Thin dotted lines indicate the expected shift in $\delta^2H_{CH_4}$ and $\delta^{13}C_{CH_4}$ caused by partial

649 aerobic methane oxidation adopting a slope of 8.5. Thick dashed lines indicate the expected shift

650 in $\delta^2H_{CH_4}$ and $\delta^{13}C_{CH_4}$ caused by oxidation with ·OH adopting a slope 75 (Saueressig et al., 2001;

651 Feisthauer et al., 2011). Mixing in $\delta^2H_{CH_4}$ vs $\delta^{13}C_{CH_4}$ space plots as a straight line, dark-red dot-

652 dashed line. Numbers represent individual caves. Note the all of the data points can be described
653 by a source of CH_4 from the atmosphere, a source from acetoclastic fermentation (S1), a source
654 from carbonate reduction (S2), mixing, and methanotrophic oxidation and do not plot within the
655 bounds of ·OH oxidization (gray and blue fields). For clarity, some points are shown as black dots
656 with a line pointing to the cave number of the sample. Error bars are not included with black circles
657 for clarity. In other locations, if error bars are not visible, they are smaller than the data points.

658

659 **Table 1:** Overview of collected data. 'Discrete' measurements refer to the laboratory.

Cave	State	Collection date[a]	Sites measured	$[CH_4]$ min (ppmv)	$[CH_4]$ max (ppmv)	$[CO_2]$ min (ppmv)	$[CO_2]$ max (ppmv)	Methods
1	AL	2015-04-07	1	NA[b]	2.2	NA	378	*In-situ*
2	IN	2013-08-10	4	0.42	1.89	2140	8000	Discrete
3	IN	2013-08-07	3	0.23	4.2	13400	17900	Discrete
4	IN	2013-06-18	2	0.3	0.7	3900	5200	Discrete
5	IN	2013-06-29	3	0.4	1.18	3300	8600	Discrete
6	IN	2013-06-14	3	0.32	1.32	750	3700	Discrete
7	KY	2012-05-05	4	0.3	0.9	3500	6020	*In-situ*
8	KY	2012-05-06	5	0.0	0.4	5200	6200	*In-situ*
9	KY	2012-05-07	7	0.08	0.6	900	1500	*In-situ*
10	KY	2013-07-18	1	NA	1.79	NA	920	Discrete
11	KY	2013-07-18	1	NA	0.91	NA	2790	Discrete
12	KY	2013-07-18	1	NA	1.37	NA	1790	Discrete
13	KY	2015-04-10	4	2.3	2.6	349	390	Mixed
14	KY	2015-04-10	3	1.82	2.33	351	390	*In-situ*
15	KY	2015-04-10	2	0.9	1.8	440	486	Mixed
16	OH	2015-04-10	1	NA	1.95	NA	940	*In-situ*
17	PA	2013-07-15	5	1.4	1.9	1430	2400	Mixed
18	PA	2013-07-15	4	0.4	1.1	760	4250	Mixed
19	PA	2013-07-15	4	0.4	0.5	900	1400	Mixed
20	PA	2013-07-16	3	0.4	1.0	3390	4240	Mixed
21	TN	2013-07-18	3	0.5	1.25	2210	2430	Mixed
22	TN	2013-07-19	3	2.6	3.5	490	1610	Mixed
23	TN	2015-04-07	7	0.2	1.02	1100	1600	Mixed
24	TN	2015-04-08	6	0.6	1.6	1100	1515	Mixed
25	TN	2015-04-09	7	0.2	0.8	1430	2100	Mixed
26	TN	2015-04-09	3	0.6	0.79	630	660	Mixed

27	VA	2015-07-17	5	0.6	1.0	6300	14700	Mixed
28	VA	2015-07-17	4	0.4	0.8	2480	7600	Mixed
29	VA	2015-07-17	5	0.4	1.6	1100	8740	Mixed
30	VA	2015-07-18	5	0.3	1.5	1090	19900	Mixed
31	VA	2015-07-18	6	0.4	2.2	410	8900	Mixed
32	NZ[c]	2014-10-04	8	1.5	2.8	500	590	*In-situ*
33	NZ	2014-10-04	3	1.0	1.7	500	620	*In-situ*
34	NZ	2014-10-04	6	1.0	1.8	500	1000	*In-situ*
35	IN	2014-06-11	2	0.14	0.3	NA[d]	NA[d]	*In-situ*
36	MO	2016-09-24	9	0.1	1.5	2590	6190	*In-situ*

[a] Dates are formatted yyyy-mm-dd

[b] NA = not applicable where only 1 sample was obtained.

[c] NZ = New Zealand

[d] NA = Only CH_4 was measured

660

661 **Table 2:** *In-situ* instrumentation used in this study.

Instrument	Maker	Location	Method	Analytes Measured	Lower detection limits
GasFinder2	Boreal Laser	Spruce Grove, Alberta Canada	Tunable Diode Laser Spectroscopy	CH_4	1 ppmv m^{-1}
Inspectra	Gazomat, WEST Systems	Pontedera, Italy	Tunable Diode Laser Spectroscopy	CH_4	0.1 ppmv
LGD F200	Axetris, SARAD	Kägiswil, Switzerland	Tunable Diode Laser Spectroscopy	CH_4	0.2 ppmv
madIR-D01 CO2	Madur, SARAD	Zgierz, Poland	Tunable Diode Laser Spectroscopy	CO_2	400 ppmv
DX4030	Gasmet	Milton Keynes, United Kingdom	Fourier Transform Infrared Spectroscopy	CH_4, CO_2, NH_3,	0.3 ppmv CH_4, 200 ppmv CO_2, 0.1 ppbv NH_3
LI820	LICOR, WEST Systems	Pontedera, Italy	Nondispersive Infrared Spectroscopy	CO_2	5 ppmv
RTM 2200	SARAD	Dresden, Germany	Alpha spectroscopy	Rn	0 Bq/m³

662